atmosphere

MDPI

Article

Effect of Werner-Type Complex Formation of Cu^{2+} and Fe^{2+} on Oxidative Potentials Assessed Using Ascorbic Acid Assay

Hideaki Sekine [1], Hikaru Ito [2] and Yoshika Sekine [1,2,*]

[1] Graduate School of Science and Technology, Tokai University, 4-1-1 Kitakaname, Hiratsuka 259-1292, Kanagawa, Japan; 3ctad017@mail.u-tokai.ac.jp
[2] Department of Chemistry, School of Science, Tokai University, 4-1-1 Kitakaname, Hiratsuka 259-1292, Kanagawa, Japan
* Correspondence: yoshika@tokai.ac.jp

Abstract: The ascorbic acid (AA) assay is a widely recognized tool for assessing the oxidation potential (OP) of atmospheric particulate matter (PM), including $PM_{2.5}$. OP quantified through the cell-free AA assay can be used to study the association between chemical properties and harmful biological effects, such as the degradation of AA in the lungs by PM sample. AA is oxidized and depleted in solutions containing redox-active species such as polycyclic aromatic hydrocarbon quinones and heavy metal ions (Cu^{2+} and Fe^{2+}), which are potential PM components. The metal ions form a Werner-type complex with ligands; thus, the AA depletion rate changes with the co-existing ligands in the PM sample. However, how the coordination structure of the complexes affects the AA depletion rate is poorly understood. This study examined the impact of the Werner-type complex formation of Cu^{2+} and Fe^{2+} on the AA depletion rate. Cu^{2+} and Fe^{2+} complexes were prepared by mixing them with three ethyleneamine forms: ethylenediamine, diethylenetriamine, and triethylenetetramine. The AA depletion rate was determined by measuring the changes in absorbance at 265 nm in the reaction solutions. Results indicated that the AA depletion rates of Cu^{2+} and Fe^{2+} were suppressed by the formation of complexes, and the degree of suppression depended on the coordination number and stability constants of the ethyleneamines. Additionally, AA depletion rates decreased with decreasing oxidative reduction potential in the solutions and changes in the coordination structures of the metal ion complexes. These findings demonstrate that the formation of Werner-type complexes with Cu^{2+} and Fe^{2+} reduces the AA depletion rate. As the number of ligands coordinating to the metal ions increases, the ORP decreases, creating a reducing environment that suppresses the oxidation of AA.

Keywords: particulate matter; metal; complex; oxidative stress; coordination structure; oxidative potential; ascorbic acid assay; ethyleneamine

check for updates

Academic Editors: Yoshizumi Kajii and Avelino Eduardo Saez

Received: 26 December 2024
Revised: 27 January 2025
Accepted: 6 February 2025
Published: 7 February 2025

Citation: Sekine, H.; Ito, H.; Sekine, Y. Effect of Werner-Type Complex Formation of Cu^{2+} and Fe^{2+} on Oxidative Potentials Assessed Using Ascorbic Acid Assay. *Atmosphere* **2025**, *16*, 192. https://doi.org/10.3390/atmos16020192

Copyright: © 2025 by the authors. Licensee MDPI, Basel, Switzerland. This article is an open access article distributed under the terms and conditions of the Creative Commons Attribution (CC BY) license (https://creativecommons.org/licenses/by/4.0/).

1. Introduction

Atmospheric particulate matter (PM) is a public health concern with significant environmental and health impacts worldwide. The adverse effects of fine PM (Particulate Matter 2.5, $PM_{2.5}$) on human health were investigated in epidemiological studies conducted in the United States in the 1990s [1–7]. Numerous studies have demonstrated associations between urban $PM_{2.5}$ concentrations and human mortality, respiratory diseases, and cardiovascular diseases [1–8]. Inhaled $PM_{2.5}$ reportedly enters the bloodstream from the lungs, allowing the redox-active substances in $PM_{2.5}$ to infiltrate cells. Inside cells, these substances promote the production of reactive oxygen species (ROS) such as superoxide

anion radical ($O_2^{\bullet-}$), hydrogen peroxide (H_2O_2), and hydroxy radical ($^{\bullet}OH$), which induce oxidative stress in a body and potentially affect health [8–11].

Chemical species contributing to ROS production include polycyclic aromatic hydrocarbon (PAH) quinones, oxidative derivatives of PAHs [9,12–14], and soluble metals such as Cu and Fe [11], which act as redox-active substances in biological systems. Therefore, the oxidative potential (OP), defined as the ability of PM to oxidize target molecules generating ROS, has been proposed as a biologically relevant exposure index to link the chemical properties of PM to human health outcomes [15–20]. The OP of PM samples has been evaluated through in vitro methods such as the ascorbic acid (AA) [16–20], DL-dithiothreitol assay [21,22], terephthalate sodium [23,24], and electron spin resonance assays [25]. AA is a physiological antioxidant in the human lung that is oxidized to dehydroascorbic acid by the redox-active substances in PM, consequently reducing these redox-active species. The reduced species in PM transfer electrons to oxygen molecules, promoting ROS formation [26]. Based on this principle, the AA assay is used to evaluate the OP of PM by assessing the rate of AA depletion upon contact with the PM constituents in an aqueous solution. The AA assay is particularly sensitive to the OP of metal ions such as Cu^{2+} and Fe^{2+}, whose toxicity has been attributed to their potential as a catalyst for oxidative damage to tissues through redox cycling, particularly in the presence of hydrogen peroxide [27,28].

Metal ions potentially form complexes with organic or inorganic ligands in PM samples. Among such complexes, those in which ligands with lone electron pairs coordinate with the central metal ions are called Werner-type complexes [29]. Cu^{2+} and Fe^{2+} serve as central metal ions, and their complexes form unique spatial structures depending on the coordination number [29]. An octahedral complex is formed when the coordination number is six. Figure 1 illustrates typical octahedral complexes of bivalent metal ions (M) with ethyleneamines, including ethylenediamine (en), diethylenetriamine (dien), and triethylenetetramine (trien). En is a bidentate ligand that coordinates up to three molecules with a single central metal ion. The tridentate dien ligand coordinates up to two molecules, whereas the tetradentate trien ligand coordinates one.

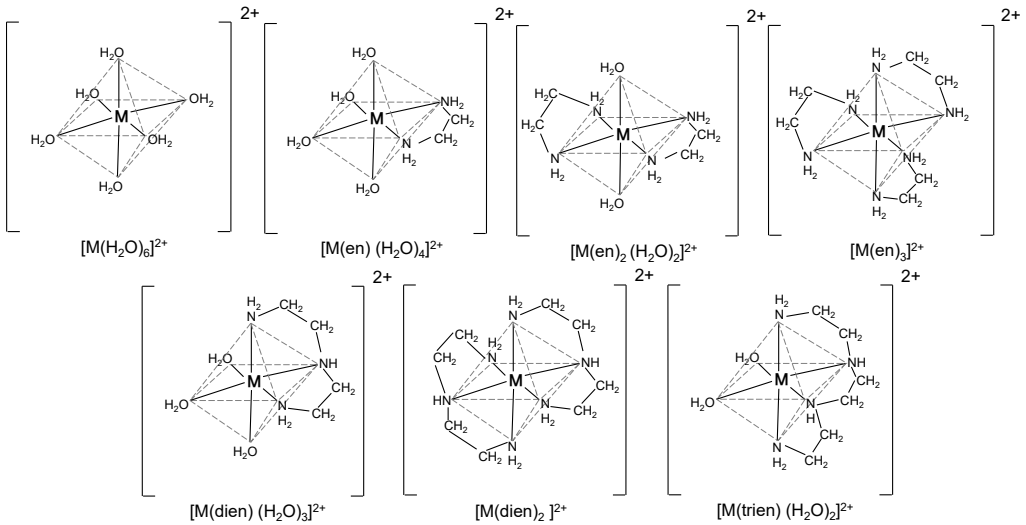


Figure 1. Typical coordination structure of octahedral complexes of bivalent metal ion and ethylenediamine (en), diethylenetriamine (dien), and triethylenetetramine (trien) ligands in aqueous solutions.

Environmental materials such as PM are complex mixtures containing various substances. Therefore, OP research should consider the concentrations of individual components and the interactions among co-existing components [30], particularly for metal ions that readily form Werner-type complexes with ligands. However, how the coordination

structure of the complexes affects the AA depletion rate is poorly understood. In this study, we aimed to elucidate the effects of the Werner-type complex formation of Cu^{2+} and Fe^{2+} on the AA depletion rate using en, dien, and trien as model ligands whose stability constants were previously known.

2. Method

2.1. Reagents

Copper (II) sulfate pentahydrate (FUJIFILM Wako Pure Chemical, Osaka, Japan, special grade, [31]) and iron (II) chloride tetrahydrate (Kanto Chemical, Tokyo, Japan, first grade, [32]) were dissolved and diluted with ultrapure water (Milli-Q ultrapure type1 water, 18.2 MΩ·cm at 298 K, Simplicity® water purification system, Merck KGaA, Darmstadt, Germany) to prepare 0.010 mM $CuSO_4$ and 1.0 mM $FeCl_2$ aqueous solutions, respectively. Ethyleneamines, including en (FUJIFILM Wako Pure Chemical, Osaka, Japan, special grade), dien (Kanto Chemical, Tokyo, Japan, first grade), and trien (Kanto Chemical, Tokyo, Japan reagent grade), were dissolved and diluted with the ultrapure water to prepare 0.010 mM and 1.0 mM solutions. Since the ability of AA depletion differed between Cu^{2+} and Fe^{2+}, as described in Section 2.4, 0.010 mM $CuSO_4$ and 1.0 mM $FeCl_2$ solutions were used for the AA assay. L-ascorbic acid (FUJIFILM Wako Pure Chemical, Osaka, Japan; special grade) was dissolved in the ultrapure water to prepare the 10 mM solution used for the AA assay. Phosphate buffer was prepared by mixing 0.10 M KH_2PO_4 (Kanto Chemical, Tokyo, Japan, special grade) and 0.10 M Na_2HPO_4 solutions (Kanto Chemical, Tokyo, Japan, special grade) in a volume ratio of 4:1 (pH 7.4).

2.2. Determination of Metal Ion Concentration Used for Testing

To determine the optimal Cu^{2+} and Fe^{2+} concentrations for evaluating the influence of coordination structures on the AA depletion rate in this study, dilution series of $CuSO_4$ (0, 0.10, 0.20, 0.30, and 0.50 μM) and $FeCl_2$ (0, 10, 20, and 100 μM) were prepared in Milli-Q ultrapure water, and the AA depletion rates were measured as described in Section 2.4.

2.3. Preparation of Metal Complexes with Different Coordination Structures

Metal complexes with different coordination structures were prepared by mixing $CuSO_4$ or $FeCl_2$ solutions with varying amounts of en, dien, or trien solutions. As the ratio of ethyleneamine ligands to metal ions increases, higher-order complexes are formed with different coordination structures. For the Cu^{2+}-en complex, six test tubes were each filled with 1.0 mL of 0.010 mM $CuSO_4$ solution. Subsequently, 0–5.0 mL of 0.010 mM en solution was added to each tube in 1.0 mL increments (Table 1), and the total volume was adjusted to 10 mL using ultrapure water. $C_{en}/C_{Cu(II)}$ refers the molar concentration ratios of en and Cu^{2+}. The Cu^{2+}-dien and Cu^{2+}-trien complexes were prepared using the same procedure. For the Fe^{2+}-en complex, six test tubes were each filled with 1.0 mL of 1.0 mM $FeCl_2$ solution. Next, 0–2.5 mL of 1.0 mM en solution was added to each tube in 0.5 mL increments, and the total volume was adjusted to 10 mL using ultrapure water. $C_{en}/C_{Fe(II)}$ are the molar concentration ratios of en and Fe^{2+}. The Fe^{2+}-dien and Fe^{2+}-trien complexes were prepared using the same approach. The ligand-to-metal ratios were determined by considering the overall stability constants to form a diverse range of coordination structures as described in Section 2.6. The metal complex formation was confirmed by observing the color change caused by d-electron transitions, which occurred rapidly after mixing.

Table 1. The mixing of Cu^{2+} and Fe^{2+} solutions with varying amounts of en solution for the preparation of the Werner-type octahedral complex of Cu^{2+}-en and Fe^{2+}-en.

Test Tube #	**0.010 mM Cu^{2+} (mL)**	**0.010 mM en (mL)**	**$C_{en}/C_{Cu(II)}$**
C-1	1.0	0	0
C-2	1.0	1.0	1.0
C-3	1.0	2.0	2.0
C-4	1.0	3.0	3.0
C-5	1.0	4.0	4.0
C-6	1.0	5.0	5.0
Test Tube #	1.0 mM Fe^{2+} (mL)	1.0 mM en (mL)	$C_{en}/C_{Fe(II)}$
F-1	1.0	0	0
F-2	1.0	0.5	0.5
F-3	1.0	1.0	1.0
F-4	1.0	1.5	1.5
F-5	1.0	2.0	2.0
F-6	1.0	2.5	2.5

2.4. Measurement of AA Depletion Rate

To prepare the test sample, 2.0 mL of each complex sample prepared in Sections 2.2 and 2.3 was diluted fivefold with the phosphate buffer. The test samples stood for 24 h at 37 °C in a thermostatic chamber. Subsequently, 0.10 mL of 10 mM L-ascorbic acid solution was added to the test sample and mixed immediately to give test solutions. The absorbance at 265 nm was measured every minute for 10 min using an Ultraviolet (UV)-Visible spectrophotometer (UVmini-1240, Shimadzu Corporation, Kyoto, Japan) using a 1.0 cm quartz cuvette. Milli-Q ultrapure water was used as a reference. Typical temporal changes in the absorbance of 0 and 0.10 μM $CuSO_4$ solution are shown in Figure 2. The test sample containing 0.10 μM $CuSO_4$ solution exhibited a significant decrease in absorbance, indicating that AA was oxidized by Cu^{2+} in the solution. The slight decrease in the ultrapure water was observed because the aqueous AA reacted with dissolved oxygen. Since the decrease in absorbance could be regarded as a straight line, the AA depletion rate was calculated using linear regression of the temporal change in absorbance at 265 nm. Using the method of Sugimoto et al. [18], the AA depletion rate (μM min^{-1}) for each test solution was determined using Equation (1):

$$AA\ depletion\ rate = -a \times \frac{N_0}{b} \quad (1)$$

where a is the slope obtained from the linear regression of the absorbance change over time, b is the intercept from the same regression, and N_0 represents the initial AA concentration of 99 μM at the time of addition. If no decrease in absorbance was observed during the 10 min assessment, the AA depletion rate was recorded as zero. Each test solution was analyzed in triplicate (n = 3).

2.5. Measurement of ORP

In general, the formation of complexes by metal ions alters their oxidation-reduction potential (redox potential, ORP) compared with that of metal ions alone owing to the ligand field effect, oxidation state stabilization, charge redistribution, and steric effect [33,34]. The ORP of each metal complex solution was measured thrice using a pen-type ORP meter (ORP70, AS ONE Corporation, Tokyo, Japan). The measurement range of the meter was ±1000 mV with ±0.2% of accuracy.

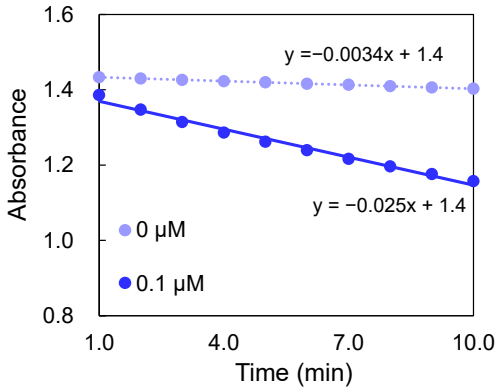


Figure 2. Typical time-courses of absorbance at 265 nm of test solution with pure water (0 μM) and 0.10 μM $CuSO_4$. Reference: Milli-Q ultrapure water.

2.6. Estimation of Coordination Structures in Sample Solutions

Following our previous study [35], the coordination structures of the Werner-type complexes in the test samples were estimated using stability constants, which are equilibrium constants used for the formation of a complex in solution [36]. As illustrated in Figure 1, en acts as a bidentate ligand and binds up to three molecules to a central metal ion. If the central metal ion is represented by M, and the bidentate ligand is denoted by L, the sequential complex formation occurs as follows:

$$\mathrm{M} + \mathrm{L} \rightleftarrows \mathrm{ML},\ K_{f1} = \frac{[\mathrm{ML}]}{[\mathrm{M}][\mathrm{L}]} \tag{2}$$

$$\mathrm{ML} + \mathrm{L} \rightleftarrows \mathrm{ML_2},\ \mathrm{K}_{f2} = \frac{[\mathrm{ML_2}]}{[\mathrm{ML}][\mathrm{L}]} \tag{3}$$

$$\mathrm{ML_2} + \mathrm{L} \rightleftarrows \mathrm{ML_3},\ K_{f3} = \frac{[\mathrm{ML_3}]}{[\mathrm{ML_2}][\mathrm{L}]} \tag{4}$$

where K_f represents the stepwise formation constant (stepwise stability constant), and the overall stability constants βi (i = 1, 2, 3) for each complex are expressed as follows:

$$\beta_1 = K_{f1} \tag{5}$$

$$\beta_2 = K_{f1} \times K_{f2} \tag{6}$$

$$\beta_3 = K_{f1} \times K_{f2} \times K_{f3} \tag{7}$$

where C_M is the total metal ion concentration. The mass balance equation for the metal ions is expressed as follows:

$$C_\mathrm{M} = [\mathrm{M}] + [\mathrm{ML}] + [\mathrm{ML_2}] + [\mathrm{ML_3}] \tag{8}$$

$$C_\mathrm{M} = [\mathrm{M}](1 + \beta_1[\mathrm{L}] + \beta_2[\mathrm{L}]^2 + \beta_3[\mathrm{L}]^3) \tag{9}$$

Substituting the expressions for the complex concentrations into the mass balance equation yields $Q_\mathrm{L} = 1 + \beta_1[\mathrm{L}] + \beta_2[\mathrm{L}]^2 + \beta_3[\mathrm{L}]^3$. Thus, the concentrations of the metal ion and each complex are expressed as below:

$$[\mathrm{M}] = \frac{1}{Q_\mathrm{L}} C_M \tag{10}$$

$$[\mathrm{ML}] = \frac{\beta_1[\mathrm{L}]}{Q_\mathrm{L}} C_\mathrm{M} \tag{11}$$

$$[ML_2] = \frac{\beta_2[L]^2}{Q_L} C_M \quad (12)$$

$$[ML_3] = \frac{\beta_2[L]^3}{Q_L} C_M \quad (13)$$

where C_L denotes the total ligand concentration. The mass balance equation for the ligands is expressed as follows:

$$C_L = [L] + [ML] + 2[ML_2] + 3[ML_3] \quad (14)$$

The coordination structures of the complexes in each sample solution were estimated by substituting the experimental ligand concentrations [L] and using the overall stability constants listed in Table 2 [37].

Table 2. Overall stability constants for the formation of octahedral complexes of Cu^{2+} and Fe^{2+} with en, dien, and trien at 298 K [35].

Ligands	Metal Ions					
	Cu^{2+}			Fe^{2+}		
	$\log\beta_1$	$\log\beta_2$	$\log\beta_3$	$\log\beta_1$	$\log\beta_2$	$\log\beta_3$
en	10.6	19.8	-	4.34	7.65	9.7
dien	15.9	20.9	-	6.23	10.36	-
trien	20.32	-	-	7.69	-	-

3. Results

3.1. Rate of AA Depletion by Metal Ions

To determine the optimal Cu^{2+} and Fe^{2+} concentrations for evaluating the influence of coordination structures on the AA depletion rate, dilution series of Cu^{2+} and Fe^{2+} were prepared, and the AA depletion rates were measured. The results are shown in Figure 3. The X-axis shows the concentration of metal ions in the test sample and the Y-axis shows the AA depletion rate. Each test was conducted thrice, and the error bars indicate the standard deviation. The AA depletion rate increased with increasing concentrations of both metal ions in the solutions. Cu^{2+} exhibited approximately three times the AA depletion rate of Fe^{2+}, even at a concentration 1/100 that of Fe^{2+}. This trend is consistent with that of previous studies on PM, which reported that Cu^{2+} has a higher rate than does Fe^{2+} [18,19]. AA reacts with dissolved oxygen in water and undergoes oxidation. The addition of Fe^{2+} and Cu^{2+} is known to accelerate the oxidation rate of AA [38]. Therefore, the depletion rate of AA increased due to the catalytic action of metal ions, depending on their concentration.

To further investigate the effect of coordination structures on the AA depletion rate during complex formation, 20 μM Fe^{2+} was selected based on the magnitude of the standard deviation, while 0.20 μM Cu^{2+}, corresponding to 1/100 of the Fe^{2+} concentration, was used.

3.2. Rate of AA Depletion by Ethyleneamines

To verify whether the use of ethyleneamines in the complex formation independently influences the oxidation of AA, the AA depletion rates of the dilution series containing only en, dien, or trien were measured (Figure 4). The X-axis shows the concentration of ligands in the test sample and the Y-axis shows the AA depletion rate. For en, no significant change in the AA depletion rate was observed at 0–0.5 μM. This indicates that en did not affect the AA depletion rate in this system. However, the AA depletion rate decreased to zero when dien and trien reacted with AA at every level. This suggests that dien and trien have antioxidant properties, presumably inhibiting the oxidation of AA by the oxygen dissolved in the solution. Although the reasons for the differences among ethyleneamines are not

clear, it is possible that the slight differences in the pH of the solution, due to the higher basicity in the order of trien > dien > en, influenced the inhibition.

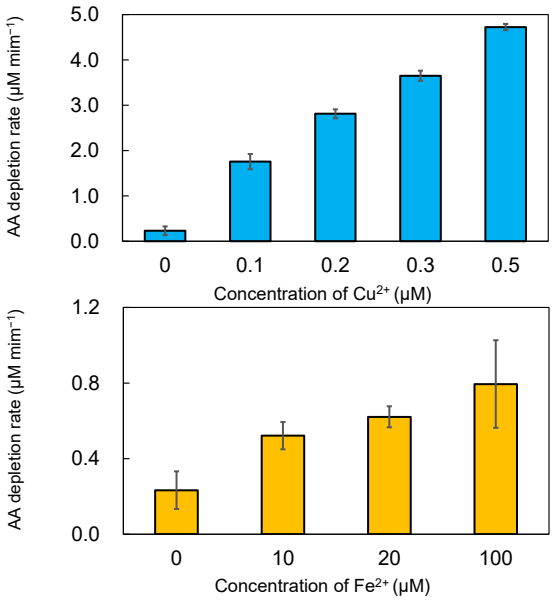


Figure 3. Relationships between the AA depletion rate and the concentration of Cu^{2+} and Fe^{2+} in the test samples. Error bars indicate the standard deviation of triplicate runs (n = 3).

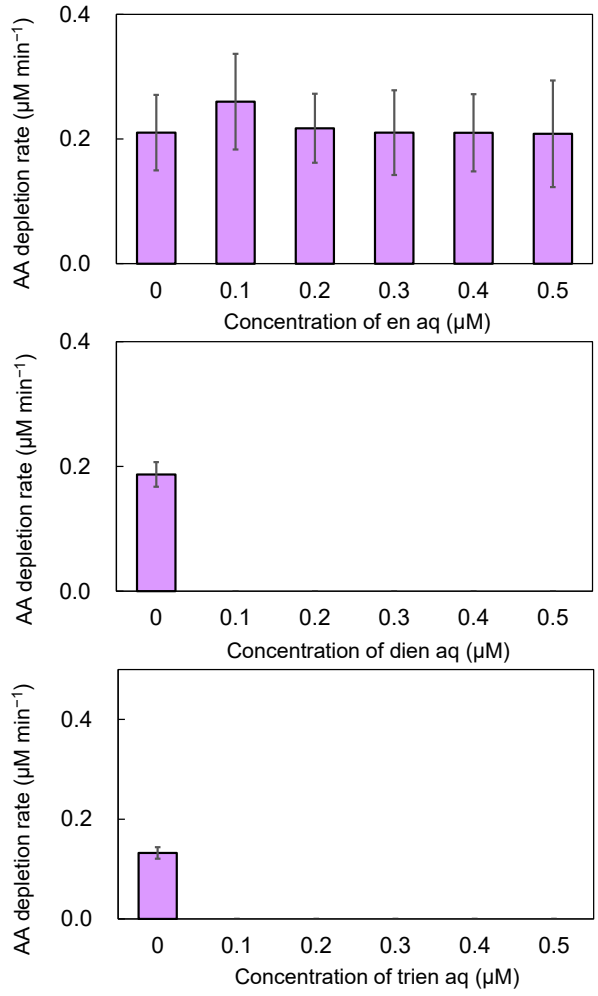


Figure 4. Relationships between the AA depletion rate and the concentrations of en, dien, and trien in the test samples. Error bars indicate the standard deviation of triplicate runs (n = 3).

3.3. Changes in the AA Depletion Rate Owing to the Formation of Cu^{2+} Complexes

The changes in the AA depletion rates in the test solutions containing 0.2 μM Cu^{2+}, along with the relative proportions of en, dien, and trien at different molar ratios, $C_{en}/C_{Cu(II)}$, were determined. The results are shown in Figure 5a. Alongside with the results, Figure 5b shows the estimated abundances of coordination structures of octahedral Cu complexes with zero, one, and two coordination numbers estimated using the overall stability constants. Although en did not affect the AA depletion rate, it suppressed the degradation of AA by Cu^{2+} through the formation of octahedral complexes. Similarly, the addition of dien and trien suppressed the AA degradation. The degree of suppression was in the order trien > dien > en. Similar to the case with ligands only in Figure 4, the en complex showed the highest AA depletion, while dien and trien exhibited significantly lower AA depletion compared to the en complex.

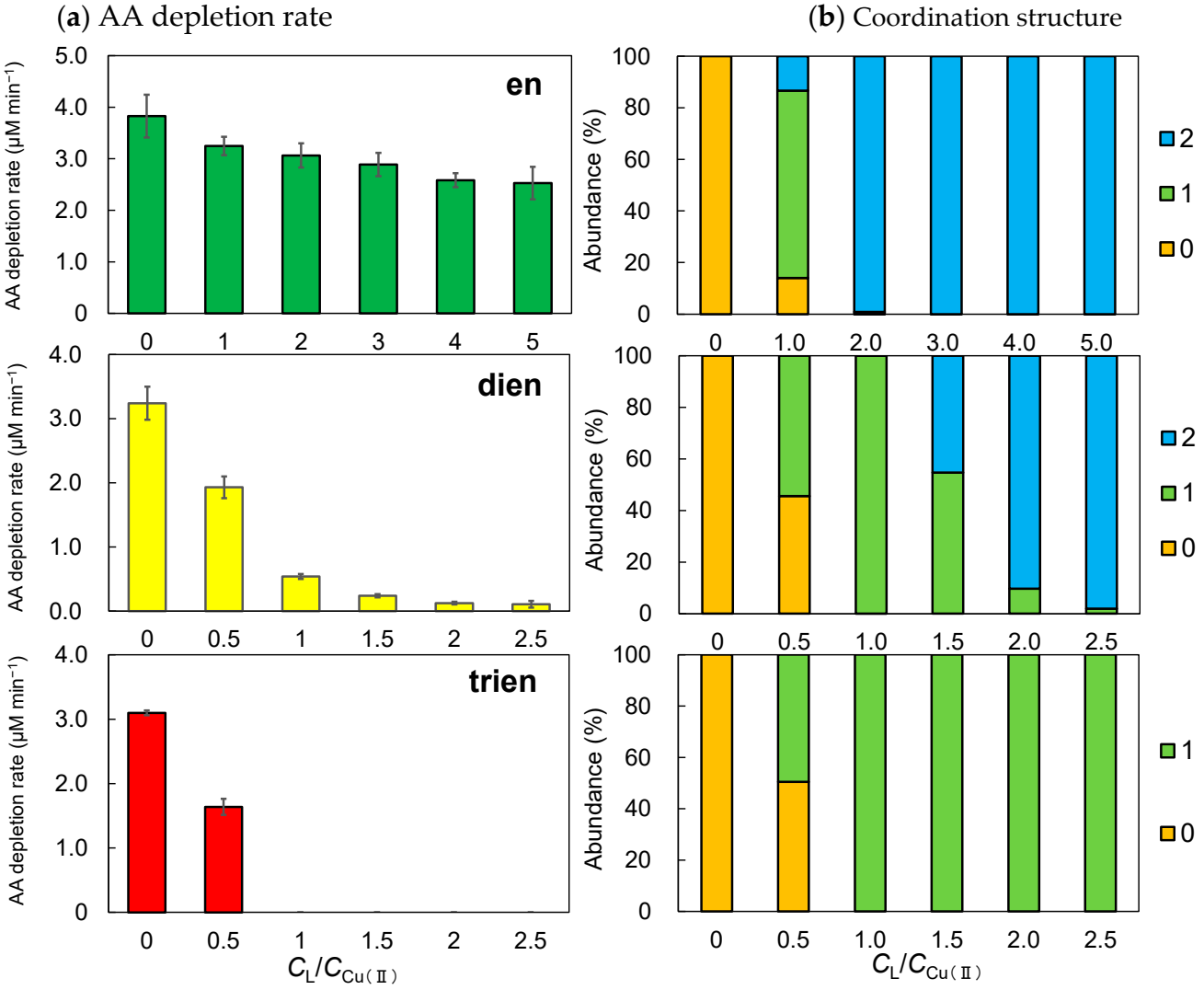


Figure 5. Variations in the AA depletion rates (n = 3) (**a**) and estimated coordination structures of octahedral metal complexes (**b**) as a function of the molar concentration ratio of ethyleneamines and bivalent metal ions, $C_L/C_{Cu(II)}$. The darker green, yellow and red show a Cu(II)-en, -dien and -trien complex, respectively. The legend in the structure graph shows the coordination number of ethyleneamines to metal ions.

3.4. Changes in the AA Depletion Rate Owing to the Formation of Fe^{2+} Complexes

Figure 6a shows the changes in the AA depletion rate in the test solutions containing 20 μM Fe^{2+}, along with the relative proportions of en, dien, and trien at different molar ratios ($C_L/C_{Fe(II)}$), and Figure 6b shows the estimated abundances of coordination structures of octahedral Fe complexes with zero, one, two, and three coordination numbers. As with the Cu^{2+} complexes, each analysis was performed thrice, and error bars represent standard deviations. The addition of ethyleneamines suppressed the decrease in AA concentration. However, the effect of ethyleneamines on the AA depletion rate for Fe^{2+} complexes was less pronounced than that for Cu^{2+} complexes. In contrast to the Cu^{2+}-trien complex, which exhibited a depletion rate of zero at a molar ratio of ≥1.0, the Fe^{2+}-trien complex did not reach zero, even though the Fe concentration was 100 times higher than that of Cu^{2+} and the trien concentration was also higher.

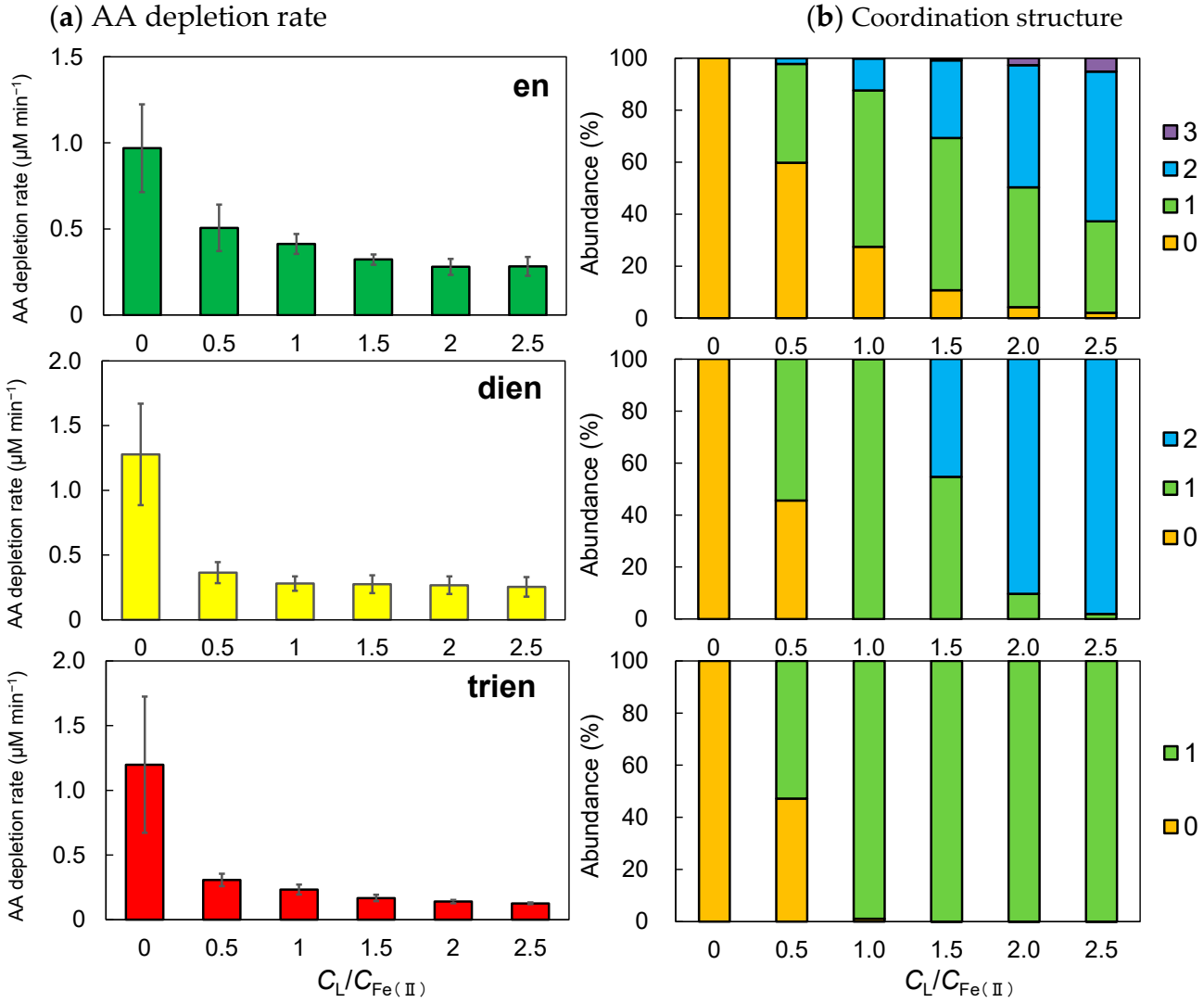


Figure 6. Variations in the AA depletion rates (n = 3) (**a**) and the estimated coordination structures of octahedral metal complexes (**b**) as a function of the molar concentration ratio of ethyleneamines and bivalent metal ions, $C_L/C_{Fe(II)}$. The darker green, yellow and red show a Fe(II)-en, -dien and -trien complex, respectively The legend in the structure graph shows the coordination number of ethyleneamines to metal ions.

4. Discussion

The AA depletion rates of Cu^{2+} and Fe^{2+} were suppressed by the formation of Werner-type octahedral complexes with ethyleneamines, and the degree of suppression depended on the coordination number. Meanwhile, the effect of ethyleneamines on the AA depletion rate for Fe^{2+} complexes was less significant compared to that for Cu^{2+} complexes. This can be attributed to the following factors:

1. Stability constants: The stability constants of the Fe^{2+}- and Cu^{2+}-trien complexes, log β_1, are 7.69 and 20.32, respectively (Table 2). The complexes with higher stability constants tended to exhibit lower oxidative activity. This observation aligns with the results of studies examining the oxidative activity of Cu^{2+} complexes with ethyleneamine derivatives [39].
2. The Jahn–Teller effect: Cu^{2+}, with its $3d^9$ electron configuration, experiences significant electrostatic repulsion with the negatively charged ligands in an octahedral complex. To stabilize the structure, it undergoes distortion from an ideal octahedral shape owing to the Jahn–Teller effect [40]. This effect causes the bond distance along one axis to become longer than that along the other two axes, resulting in a unique coordination structure. This specific structural characteristic may explain the differences in the AA depletion rates compared with those of Fe^{2+} complexes.
3. Catalytic activity of Cu^{2+}: Cu^{2+} acts catalytically, being reduced to Cu^{+} by AA. The Cu^{+} reacts with O_2 to produce hydrogen peroxide, which is subsequently re-oxidized to Cu^{2+} [41]. Similarly, the Cu^{+} species generates highly reactive $^{\bullet}OH$ radicals through Fenton-like reactions with hydrogen peroxide [42]. The complexation of Cu^{2+} by trien possibly prevented its reduction by AA, suppressing AA oxidation. Furthermore, the antioxidant properties of trien may have inhibited AA oxidation.

Regarding the decrease in the AA depletion rate accompanying the complexation of Cu^{2+} and Fe^{2+}, Figure 7 shows the relationship between the ORP and the AA depletion rate of each metal complex solution. The AA depletion rate of the Cu^{2+}-en and Cu^{2+}-trien showed a linear relationship with the ORP of the solution (r^2 = 0.96 for en, and r^2 = 0.94 for dien) (Figure 7a). A similar trend was observed for trien with the greater suppression at zero rates. Similarly, the linear relationships were observed for Fe complexes, except trien (Figure 7b). This aligns with previous findings that the oxidation rate of AA slows when Cu^{2+} and Fe^{2+} ions are chelated with ligands [43,44]. These results indicate that the coordination structure alters the ORP of the solution, leading to changes in the AA depletion rate; as the number of ligands coordinating to the metal ions increases, the ORP decreases, creating a reducing environment that suppresses the oxidation of AA. Nevertheless, actual PM samples contain various types of ligands that combine with metal ions. In the hazard assessment of PM samples, determining the concentrations of individual chemical components is crucial, as chemical components may easily bind, as in the Werner-type complex. Consequently, mixed toxicity assessment methods, such as measurement of OP based on the AA assay, are essential.

The limitation of this study is that it focuses on model complexes generated from Cu^{2+} or Fe^{2+} and three ethyleneamines. PM contains not only Cu and Fe but also other metals including Pb, Zn, Ni, Mn Cr, Ti, Ca, Mg, K, Na, Si, and Al [18] and ligands such as acetate, formate, oxalate, and other humic-like substances [45]. Fe^{2+} and Cu^{2+} act as catalysts that accelerate the air oxidation of AA, while the catalytic ability of metal ions other than Fe and Cu on AA remains unknown. Thus, it is important to extend the investigation to other combinations considering the coordination structure and ORP associated with complex formation.

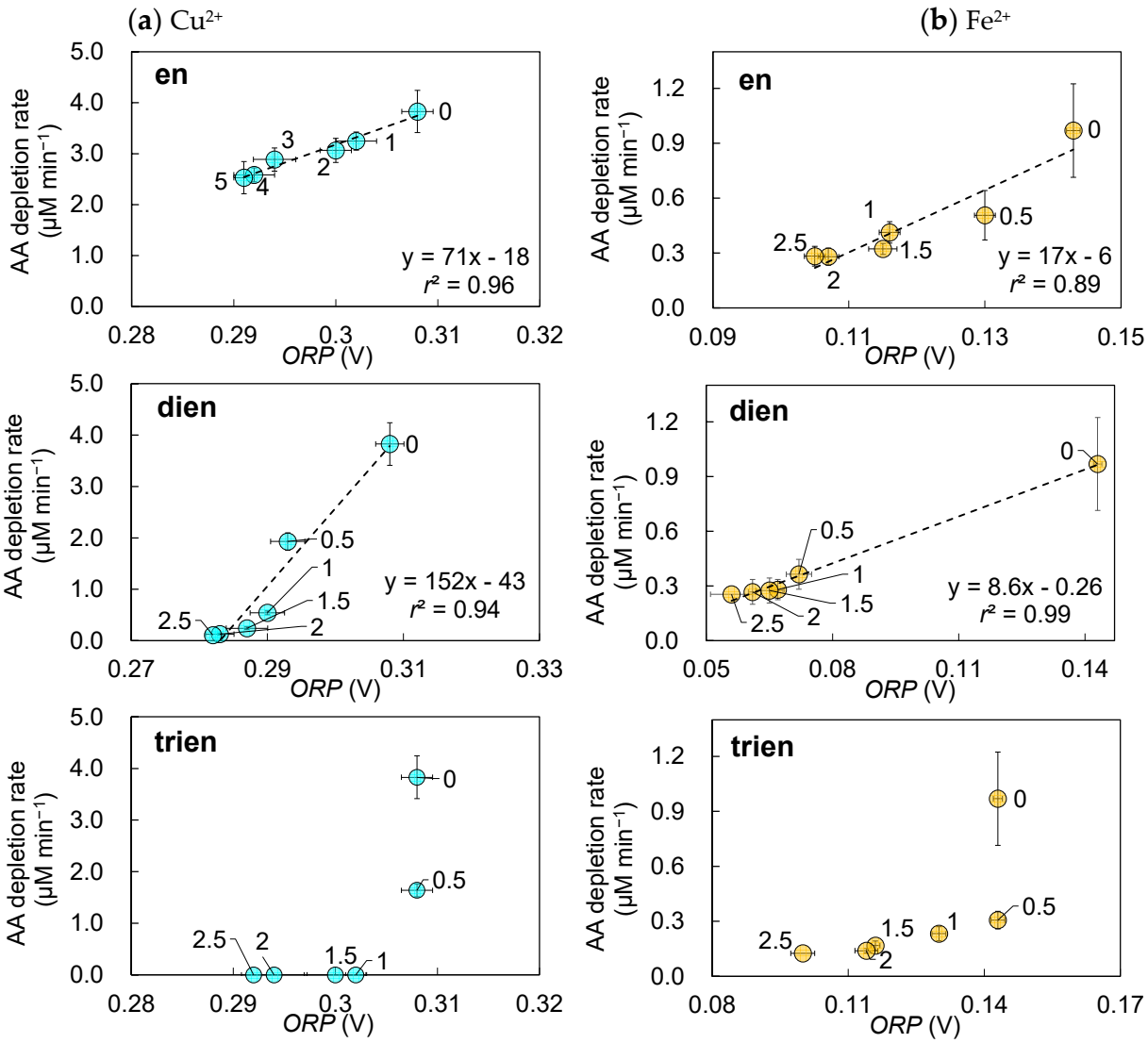


Figure 7. Relationships between *ORP* and AA depletion rate for each ethyleneamine complex. Numbers alongside plots are molar ratios of C_L/C_M in reaction solution. (**a**,**b**) show a Cu(II), Fe(II) complex, respectively.

5. Conclusions

The AA assay is used to evaluate the OP of PM samples. This study aimed to elucidate the effect of the Werner-type complex formation of Cu^{2+} and Fe^{2+} with en, dien, and trien on the AA depletion rate. The results showed that the AA depletion rates of Cu^{2+} and Fe^{2+} were suppressed by the formation of octahedral complexes, a phenomenon influenced by the coordination number and stability constants of the ligands. The AA depletion rate was also affected by the ORP in the solution, because the formation of complexes resulted in a decrease in ORP, creating a more reducing environment, which made AA less susceptible to air oxidation. Similarly, the coordination structure altered the ORP of the solution, leading to changes in the AA depletion rate. PM samples contain various ligands that can combine with metal ions. In the hazard assessment of PM samples, understanding the concentrations of the individual chemical components is crucial. These components easily bind to form complexes, such as the Werner-type complexes. Therefore, mixed toxicity assessment methods, such as OP-based AA assays, are essential because PM is a mixture that, when inhaled, oxidizes AA in the lungs, reducing the body's ability to eliminate ROS.

Author Contributions: Conceptualization, H.S. and Y.S.; methodology, H.I.; writing—original draft preparation, H.S.; writing—review and editing, H.S.; visualization, H.S.; supervision, Y.S. All authors have read and agreed to the published version of the manuscript.

Funding: This research received no external funding.

Institutional Review Board Statement: Not applicable.

Informed Consent Statement: Not applicable.

Data Availability Statement: The data presented in this study are available within the article.

Conflicts of Interest: The authors declare no conflicts of interest.

References

1. Dockery, D.W.; Pope, D.C.A., III; Xu, X.; Spengler, J.D.; Ware, J.H.; Fay, M.E.; Ferris, B.G.; Speizer, F.E. An association between Air Pollution and Mortality in Six U.S. Cities. *N. Engl. J. Med.* **1993**, *329*, 1753–1759. [CrossRef] [PubMed]
2. Krewski, D.; Burnett, R.T.; Goldberg, M.S.; Hoover, K.; Siemiatycki, J.; Abrahamowicz, M.; White, W.H. Validation of the Harvard Six Cities Study of particulate air pollution and mortality. *N. Engl. J. Med.* **2004**, *350*, 198–199. [CrossRef] [PubMed]
3. Laden, F.; Schwartz, J.; Speizer, F.E.; Dockery, D.W. Reduction in fine particulate air pollution and mortality: Extended follow-up of the Harvard Six Cities study. *Am. J. Respir. Crit. CareMed.* **2006**, *173*, 667–672. [CrossRef] [PubMed]
4. Pope, D.C.A., III; Thun, M.J.; Namboodiri, M.M.; Dockery, D.W.; Evans, J.S.; Speizer, F.E.; Heath, C.W., Jr. Particulate air pollution as a predictor of mortality in a prospective study of U.S. adults. *Am. J. Respir. Crit. CareMed.* **1995**, *151*, 669–674. [CrossRef]
5. Pope, D.C.A., III; Burnett, R.T.; Thun, M.J.; Calle, E.E.; Krewski, D.; Ito, K.; Thurston, G.D. Lung cancer, cardiopulmonary mortality, and long-term exposure to fine particulate air pollution. *J. Am. Med. Assoc.* **2002**, *287*, 1132–1141. [CrossRef]
6. Pope, D.C.A., III; Burnett, R.T.; Thurston, G.D.; Thun, M.J.; Calle, E.E.; Krewski, D.; Godleski, J.J. Cardiovascular mortality and long-term exposure to particulate air pollution: Epidemiological evidence of general pathophysiological pathways of disease. *Circulation* **2004**, *109*, 71–77. [CrossRef]
7. Krewski, D.; Jerrett, M.; Burnett, R.T.; Ma, R.; Hughes, E.; Shi, Y.; Turner, M.C.; Pope, D.C.A., III; Thurston, G.; Calle, E.E.; et al. Extended follow-up and spatial analysis of the American Cancer Society study linking particulate air pollution and mortality. *Res. Rep. Health Eff. Inst.* **2009**, *140*, 5–136. Available online: https://www.researchgate.net/publication/26690365_Extended_Follow-Up_and_Spatial_Analysis_of_the_American_Cancer_Society_Study_Linking_Particulate_Air_Pollution_and_Mortality (accessed on 23 January 2025).
8. Brook, R.D.; Rajagopalan, S.; Pope, D.C.A., III; Brook, J.R.; Bhatnagar, A.; Diez-Roux, A.V.; Holguin, F.; Hong, Y.; Luepker, R.V.; Mittleman, M.A.; et al. Particulate matter air pollution and cardiovascular disease: An update to the scientific statement from the American Heart Association. *Circulation* **2010**, *121*, 2331–2378. [CrossRef]
9. Squadrito, G.L.; Cueto, R.; Dellinger, B.; Pryor, W.A. Quinoid redox cycling as a mechanism for sustained free radical generation by inhaled airborne particulate matter. *Free Radic. Biol. Med.* **2001**, *31*, 1132–1138. [CrossRef]
10. Cho, A.K.; Sioutas, C.; Miguel, A.H.; Kumagai, Y.; Schmitz, D.A.; Singh, M.; Eiguren-Fernandez, A.; Froines, J.R. Redox activity of airborne particulate matter at different sites in the Los Angeles Basin. *Environ. Res.* **2005**, *99*, 40–47. [CrossRef]
11. Charrier, J.G.; Anastasio, C. On dithiothreitol (DTT) as a measure of oxidative potential for ambient particles: Evidence for the importance of soluble transition metals. *Atmos. Chem. Phys.* **2012**, *12*, 11317–11350. [CrossRef] [PubMed]
12. Kishikawa, N.; Ohkubo, N.; Ohyama, K.; Nakashima, K.; Kuroda, N. Chemiluminescence assay for quinones based on generation of reactive oxygen species through the redox cycle of quinone. *Anal. Bioanal. Chem.* **2008**, *393*, 1337–1343. [CrossRef]
13. Sugimoto, R.; Kumagai, Y.; Nakai, Y.; Ishii, T. 9,10-Phenanthraquinone in diesel exhaust particles downregulates Cu, Zn-SOD and HO-1 in human pulmonary epithelial cells: Intracellular iron scavenger 1,10-phenanthroline affords protection against apoptosis. *Free Radic. Biol. Med.* **2005**, *38*, 388–395. [CrossRef] [PubMed]
14. Motoyama, Y.; Bekki, K.; Chung, S.W.; Tang, N.; Kameda, T.; Toriba, A.; Taguchi, K.; Hayakawa, K. Oxidative Stress More Strongly Induced by ortho- Than para-quinoid Polycyclic Aromatic Hydrocarbons in A549 Cells. *J. Health Sci.* **2009**, *55*, 845–850. [CrossRef]
15. Visentin, M.; Pagnoni, A.; Sarti, E.; Pietrogrande, M.C. Urban $PM_{2.5}$ oxidative potential: Importance of chemical species and comparison of two spectrophotometric cell-free assays. *Environ. Pollut.* **2016**, *19*, 72–79. [CrossRef]
16. Mudway, I.S.; Stenfors, N.; Duggan, S.T.; Roxborough, H.; Zielinski, H.; Marklund, S.L.; Blomberg, A.; Frew, A.J.; Sandström, T.; Kelly, F.J. An in vitro and in vivo investigation of the effects of diesel exhaust on human airway lining fluid antioxidants. *Arch. Biochem. Biophys.* **2004**, *423*, 200–212. [CrossRef]
17. Fang, T.; Verma, V.; Bates, J.T.; Abrams, J.; Klein, M.; Strickland, M.J.; Sarnat, S.E.; Chang, H.H.; Mulholland, J.A.; Tolbert, P.E.; et al. Oxidative potential of ambient water-soluble $PM_{2.5}$ in the southeastern United States: Contrasts in sources and health associations between ascorbic acid (AA) and dithiothreitol (DTT) assays. *Atmos. Chem. Phys.* **2016**, *16*, 3865–3879. [CrossRef]

18. Sugimoto, K.; Okuda, T.; Hasegawa, S.; Nishita, C.; Hara, K.; Hayashi, M. Examination of the Oxidation Mechanism of Ascorbic Acid When Measuring Oxidative Potential Using the Ascorbic Acid Assay. *J. Jpn. Soc. Atmos. Environ.* **2021**, *56*, 96–107. [CrossRef]
19. Pietrogrande, M.C.; Bertoli, I.; Manarini, F.; Russo, M. Ascorbate assay as a measure of oxidative potential for ambient particles: Evidence for the importance of cell-free surrogate lung fluid composition. *Atmos. Environ.* **2019**, *211*, 103–112. [CrossRef]
20. Dubey, S.; Vijay, P.; Raparthi, N.; Phuleria1, H.C. Investigating $PM_{2.5}$ Oxidative Potential and Its Association with Chemical Constituents Measured outside of Urban Residences in Three Metropolitan Cities of India. *J. Health Pollut.* **2024**, *12*, 1–4. [CrossRef]
21. Misawa, K.; Sohara, K.; Kumai, Y.; Sekine, Y. Photocatalytic reduction of oxidative potential of particulate matter 2.5 ($PM_{2.5}$). *Indoor Environ.* **2019**, *22*, 15–22. [CrossRef]
22. Guo, H.; Jin, L.; Huang, S. Effect of PM characterization on PM oxidative potential by acellular assays: A review. *Rev. Environ. Health* **2020**, *35*, 461–470. [CrossRef] [PubMed]
23. Sohara, K.; Yamauchi, K.; Sekine, Y. Evaluation of ·OH Production Potential of Particulate Matter ($PM_{2.5}$) Collected on TiO2-Supporting Quartz Filters. *Catalysts* **2022**, *12*, 1016. [CrossRef]
24. Xiong, Q.; Yu, H.; Wang, R.; Wei, J.; Verma, V. Rethinking Dithiothreitol-Based Particulate Matter Oxidative Potential: Measuring Dithiothreitol Consumption versus Reactive Oxygen Species Generation. *Environ. Sci. Technol.* **2017**, *51*, 6507–6514. [CrossRef]
25. Shi, T.; Schins, R.P.F.; Knaapen, A.M.; Kuhlbusch, T.; Pitz, M.; Heinrich, J.; Borm, P.J.A. Hydroxyl radical generation by election paramagnetic resonance as a new method to monitor ambient particulate matter composition. *J. Environ. Monit.* **2003**, *5*, 550–556. [CrossRef]
26. Zielinski, H.; Mudway, I.S.; Bérubé, K.A.; Murphy, S.; Richards, R.; Kelly, F.J. Modeling the interactions of particulates with epithelial lining fluid antioxidants. *Am. J. Physiol.* **1999**, *27*, L719–L726. [CrossRef]
27. Ayres, J.G.; Borm, P.; Cassee, F.R.; Castranova, V.; Donaldson, K.; Ghio, A.; Harrison, R.M.; Hider, R.; Kelly, F.; Kooter, I.M.; et al. Evaluating the toxicity of airborne particulate matter and nanoparticles by measuring oxidative stress potential–a workshop report and consensus statement. *Inhal. Toxicol.* **2008**, *20*, 75–99. [CrossRef]
28. Perronea, M.R.; Bertolib, I.; Romanoa, S.; Russob, M.; Rispolia, G.; Pietrograndeb, M.C. $PM_{2.5}$ and PM_{10} oxidative potential at a Central Mediterranean Site: Contrasts between dithiothreitol- and ascorbic acid-measured values in relation with particle size and chemical composition. *Atmos. Environ.* **2019**, *210*, 143–155. [CrossRef]
29. Ehnbom, A.; Ghosh, S.K.; Lewis, K.G.; Gladysz, J.A. Octahedral Werner complexes with substituted ethylenediamine ligands: A stereochemical primer for a historic series of compounds now emerging as a modern family of catalysts. *Chem. Soc. Rev.* **2016**, *45*, 6799. [CrossRef]
30. Bates, J.T.; Ting, F.; Verma, V.; Zeng, L.; Weber, R.J.; Tolbert, P.E.; Abrams, J.Y.; Sarnat, S.E.; Klein, M.; Mulholland, J.A.; et al. Review of Acellular Assays of Ambient Particulate Matter Oxidative Potential: Methods and Relationships with Composition, Sources, and Health Effects. *Environ. Sci. Technol.* **2019**, *53*, 4003–4019. [CrossRef]
31. Copper Sulfate Pentahydrate. Available online: https://pubchem.ncbi.nlm.nih.gov/compound/Copper-sulfate-pentahydrate (accessed on 23 January 2025).
32. Iron Dichloride Tetrahydrate. Available online: https://pubchem.ncbi.nlm.nih.gov/compound/Iron-dichloride-tetrahydrate (accessed on 23 January 2025).
33. Van Gaal, H.L.M.; Van der Linden, J.G.M. Trends in redox potentials of transition metal complexes. *Coord. Chem. Rev.* **1982**, *47*, 41–45. [CrossRef]
34. Hawkins, C.J.; Perrin, D.D. Oxidation–reduction potentials of metal complexes in water: Some copper complexes. *J. Chem. Soc.* **1962**, 1351–1357. [CrossRef]
35. Sekine, H.; Ikeda, S.; Sekine, Y. Effect of coordination structure of Werner-type metal complexes on bioluminescence intensity of marine luminescent bacterium vibrio fischeri. *J. Environ. Chem.* **2021**, *31*, 23–29. [CrossRef]
36. Guenther, W.B. *Chemical Equilibrium*, 1st ed.; Springer: New York, NY, USA, 1975; pp. 119–139. [CrossRef]
37. Smith, R.M.; Martell, A.E. *Critical Stability Constants Volume 2: Amines*, 1st ed.; Springer: New York, NY, USA, 1975; pp. 36–111. [CrossRef]
38. Khan, M.M.; Martell, A.E. Metal ion and metal chelate catalyzed oxidation of ascorbic acid by molecular oxygen. I. Cupric and ferric ion catalyzed oxidation. *J. Am. Chem. Soc.* **1967**, *89*, 4176–4185. [CrossRef]
39. Kushioka, K. Autoxidation of Phenols catalysed by Copper-Amine Complexes (Part II)–Copper (II)–Ethylenediamine Complexes-. *J. Food Sci. Kyoto Women's Univ.* **1981**, *36*, 29–34. Available online: http://hdl.handle.net/11173/1280 (accessed on 23 January 2025).
40. Hathaway, B.J.; Billing, D.E. The electronic properties and stereochemistry of mono-nuclear complexes of the copper (II) ion. *Coord. Chem. Rev.* **1970**, *5*, 143–207. [CrossRef]
41. Ito, S.; Yamamoto, T.; Tokushige, Y. Valence change of copper in catalytic oxidation of l-ascorbic acid by molecular oxygen. *Chem. Lett.* **1980**, *9*, 1411–1414. [CrossRef]
42. Moffettt, J.W.; Zika, R.G. Reaction kinetics of hydrogen peroxide with copper and iron in seawater. *Environ. Sci. Technol.* **1987**, *21*, 804–810. [CrossRef]

43. Khan, M.M.; Martell, A.E. Metal ion and metal chelate catalyzed oxidation of ascorbic acid by molecular oxygen. II. Cupric and ferric chelate catalyzed oxidation. *J. Am. Chem. Soc.* **1967**, *26*, 7104–7111. [CrossRef]
44. Balcerczyk, A.; Sowa, K.; Bartosz, G. Metal chelators react also with reactive oxygen and nitrogen species. *Biochem. Biophys. Res. Commun.* **2007**, *352*, 522–525. [CrossRef]
45. Paris, R.; Desboeufs, K.V. Effect of atmospheric organic complexation on iron-bearing dust solubility. *Atmos. Chem. Phys.* **2023**, *13*, 4895–4905. [CrossRef]

Disclaimer/Publisher's Note: The statements, opinions and data contained in all publications are solely those of the individual author(s) and contributor(s) and not of MDPI and/or the editor(s). MDPI and/or the editor(s) disclaim responsibility for any injury to people or property resulting from any ideas, methods, instructions or products referred to in the content.